Eur Biophys J (2005) 34: 42–51
DOI 10.1007/s00249-004-0423-2

ARTICLE

Paolo Tammaro · Sergey V. Smirnov · Oscar Moran

Effects of intracellular magnesium on Kv1.5 and Kv2.1 potassium channels

Received: 25 March 2004 / Revised: 9 May 2004 / Accepted: 19 May 2004 / Published online: 8 July 2004

Abstract We characterized the effects of intracellular Mg^{2+} (Mg^{2+}_i) on potassium currents mediated by the Kv1.5 and Kv2.1 channels expressed in *Xenopus* oocytes. Increase in Mg^{2+}_i caused a voltage-dependent block of the current amplitude, apparent acceleration of the current kinetics (explained by a corresponding shift in the steady-state activation) and leftward shifts in activation and inactivation dependencies for both channels. The voltage-dependent block was more potent for Kv2.1 [dissociation constant at 0 mV, $K_d(0)$, was ~70 mM and the electric distance of the Mg^{2+} binding site, δ, was 0.2] than for the Kv1.5 channel [$K_d(0)$~40 mM and $\delta = 0.1$]. Similar shifts in the voltage-dependent parameters for both channels were described by the Gouy-Chapman formalism with the negative charge density of 1 e^-/100 Å^2. Additionally, Mg^{2+}_i selectively reduced a non-inactivating current and increased the accumulation of inactivation of the Kv1.5, but not the Kv2.1 channel. A potential functional role of the differential effects of Mg^{2+}_i on the Kv channels is discussed.

Keywords Potassium channels · Patch-clamp · Intracellular Mg^{2+} · Kv1.5 · Kv2.1

P. Tammaro · S. V. Smirnov
Dept. of Pharmacy and Pharmacology,
University of Bath, Bath, BA2 7AY, UK

O. Moran (✉)
Istituto di Biofisica, CNR, Via DeMarini 6,
16149 Genova, Italy
E-mail: moran@ge.ibf.cnr.it
Tel.: +39-010-6475558
Fax: +39-010-6475500

Present address: P. Tammaro
University Laboratory of Physiology,
Parks Road, Oxford, OX1 3PT, UK

Introduction

Changes in the extra- or intracellular concentration of divalent cations alter ion channel activity by interacting with the ion permeation mechanism (e.g. via a blockade of the channel pore) and by modulating ion channel gating (e.g. via a shift in voltage-dependent characteristics such as steady-state activation and inactivation) (Hille 2001). The interaction of extracellular Ca^{2+} and Ba^{2+} (or Sr^{2+}) within the pore of the voltage-dependent Ca^{2+} channel leads to anomalous mole fraction effect, reducing the current when both permeable cations are present in the external solution (Friel and Tsien 1989), while intracellular divalent cations can directly block Na^+ channels (Pusch et al. 1989; Pusch 1990; Lin et al. 1991).

Potassium channels can also be inhibited by intracellular cations, particularly Mg^{2+} (which is the predominant intracellular divalent cation), causing the phenomenon of inward rectification. Mg^{2+}-dependent inward rectification of the inward rectifier K^+ channels at membrane potentials more positive than the K^+ equilibrium potential has been well characterized and is believed to be due to an open channel block by Mg^{2+} driven into the inner channel mouth by membrane depolarization, thus reducing K^+ efflux (reviewed in Matsuda 1991). The investigation of the effect of intracellular Mg^{2+} on the cloned voltage-gated K^+ (Kv) channels expressed in *Xenopus* oocytes revealed strong inward rectification at membrane potentials greater than +50 mV via a mechanism which is thought to be reminiscent of the open channel block of inward rectifier channels by Mg^{2+}_i (Ludewig et al. 1993; Slesinger et al. 1993; Lopatin and Nichols 1994; Harris and Isacoff 1996; Gomez-Hernandez et al. 1997).

In animal cells an increase in Mg^{2+}_i, in addition to blocking the Kv current (Tarr et al. 1989), modulates channel gating by shifting voltage-dependent characteristics to more negative membrane potential (Perozo and Bezanilla 1991; Tammaro and Smirnov 2003). The effect

on the Kv channel gating was greatly dependent on the type of cells studied. For example, in vascular smooth muscle cells, activation and inactivation of Kv currents were altered differently by $Mg^{2+}{}_i$ (Tammaro and Smirnov 2003), while little effect on the Kv activation was observed in frog atrial myocytes (Tarr et al. 1989). In the squid axon, on the other hand, similar negative shifts in the steady-state activation and inactivation parameters were observed and explained by electrostatic interactions of $Mg^{2+}{}_i$ with negative charges seen by the voltage sensor of the K^+ channel. The effects were phosphorylation dependent (Perozo and Bezanilla 1991). It is not known, however, whether the observed differences in native cells are due to expression of different Kv channel isoforms which respond differently to changes in $Mg^{2+}{}_i$ or whether they are mediated by Mg^{2+}-dependent intracellular processes. Therefore, we investigated the effects of $Mg^{2+}{}_i$ on two different Kv channel isoforms, Kv1.5 and Kv2.1, expressed in *Xenopus* oocytes. It should be mentioned that, to the best of our knowledge, although the effects of intracellular Mg^{2+} on Kv channels have been investigated for several Kv channel isoforms, they have never been described for the Kv1.5 channel.

Materials and methods

Plasmids containing cDNA coding for Kv1.5 (Snyders et al. 1993) and Kv2.1 (Frech et al. 1989) were linearized with Not-1 (Promega, Madison, WI, USA). cRNAs were synthesized in vitro, using the SP6 mMessage mMachine kit (Ambion, Austin, Texas, USA). Defoliculated *Xenopus laevis* oocytes were injected with ~50 nl of cRNA for the Kv1.5 or Kv2.1 channel, and incubated at 18 °C for 2–5 days.

Kv currents were recorded with the conventional patch-clamp technique (Hamill et al. 1981) with an Axopatch-200 amplifier. Macroscopic currents were measured in inside-out membrane patches with aluminum silicate pipettes yielding resistance of 2–3 MΩ when filled with the pipette (extracellular) solution containing (in mM): NaCl 112.5, KCl 2.5, $CaCl_2$ 1.8, HEPES 10; pH 7.4. The bath (intracellular) solution contained (in mM): KCl 120, $MgCl_2$ 0, Tris-HCl 20, EGTA 2; pH 7.4. When the concentration of $MgCl_2$ was increased to 5 and 10 mM, the concentration of Tris-HCl was equimolarly decreased. EGTA (2 mM) was used to prevent the activation of endogenous Ca^{2+}-activated Cl^- conductance. The output of the patch-clamp amplifier was filtered with a built-in four-pole low-pass Bessel filter with a cut-off frequency of 5 kHz, and sampled at 20 kHz. Pulse stimulation and data acquisition used a 16-bit DA converter AD (ITC-16, Instrutech) controlled with a personal computer with Pulse software (Heka Electronik). Membrane patches were continually perfused with the bath solution via a nine-barrel rapid-switch perfusion system at a flow rate of 0.5–1.5 ml/min (Rapid Solution Changer, Biologic Science Instruments). Experiments were performed at a controlled temperature of 20 ± 0.5 °C. Leak and capacitive currents were subtracted on-line by using a standard P/4 method. Membrane patches were kept at the holding potential of −100 and −120 mV for Kv1.5 and Kv2.1 respectively. All recordings were obtained at least 3 min after establishing the inside-out configuration, since we noticed that this time is required for stabilization of the voltage-dependent properties of the channels. It should be noted that Kv2.1 currents demonstrated a rundown after patch excision, a phenomenon also observed by others (Lopatin and Nichols 1994). The rundown of the Kv1.5 current was less prominent. Therefore, only patches where current amplitude decreased by less than 30% within 10–20 min were used for subsequent analysis. Also, to minimize a possible effect of rundown, usually only two different concentrations of Mg^{2+} were tested with the same patch.

Data were analyzed with the program ANA (kindly provided by Dr. M. Pusch, IBF-CNR), Origin 6.02 (Microcal Software, Northhampton, MA) and with in-house software written in the Igor (Wavemetrics, Lake Oswego, OR, USA) environment. Values of the free-Mg^{2+} concentration in the intracellular solution were calculated with the program Maxchelator (Stanford University, CA, USA). Data are given as mean ± SEM (standard error of the mean) unless stated otherwise. Statistical significance was evaluated using paired or unpaired two-tailed Student *t*-test. A probability value of $P < 0.05$ was taken as the criteria for a significant difference.

Results

Effect of $Mg^{2+}{}_i$ on Kv1.5 and Kv2.1 channel currents

Heterologous expression of the Kv1.5 and Kv2.1 channels yielded fast- and slow-activating K^+ currents respectively (Fig. 1), similar to the currents described previously (Hoshi et al. 1991; Klemic et al. 1998; Kerschensteiner et al. 2003). To take into account the difference in current activation kinetics, Kv1.5 and Kv2.1 currents were measured with 50- and 100-ms voltage steps applied between −35 and +25 mV (5-mV increments) and between −50 and +50 mV (10-mV increments), respectively. An increase in $Mg^{2+}{}_i$ caused two effects on both currents: an inhibition of the current amplitude (due to a Mg^{2+}-dependent block of the channels described below in the text) and acceleration of the current activation kinetics (Figs. 1 and 2A, C). The effect of $Mg^{2+}{}_i$ was fully reversible (not shown). To compare the difference in the rate of current activation for various concentrations of $Mg^{2+}{}_i$ over the range of membrane potentials, the rise-time to the half-maximum current ($t_{1/2}$) was used. Figure 2B, D compares the difference in the mean $t_{1/2}$ measured at various membrane potentials for Kv1.5 and Kv2.1 currents in the absence and presence (shown as grey lines) of 10 mM Mg^{2+}. The

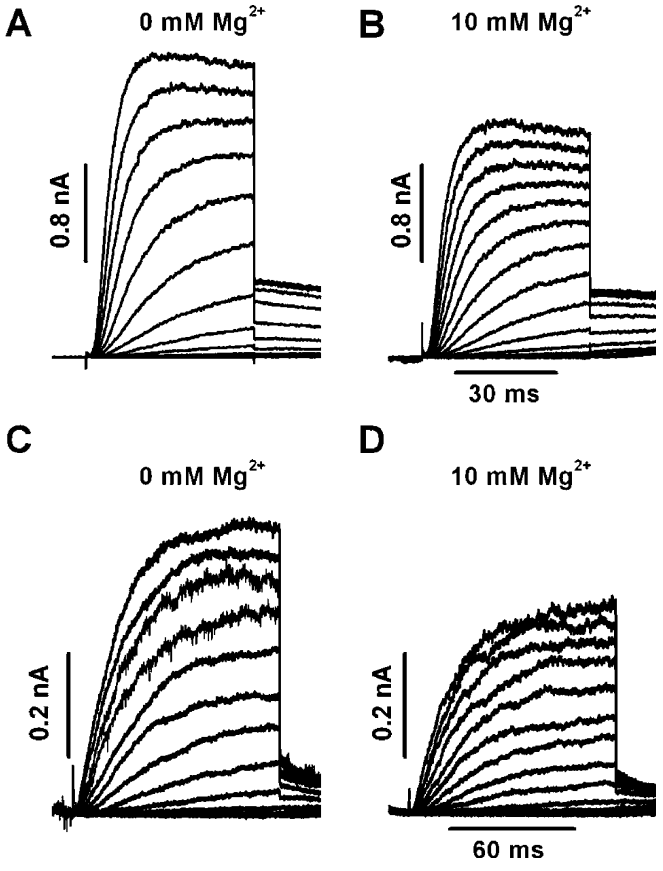

Fig. 1A–D Effect of 0 and 10 mM $Mg^{2+}{}_i$ on Kv1.5 and Kv2.1 channel currents. Families of Kv1.5 (**A**, **B**) and Kv2.1 (**C, D**) currents from representative membrane patches recorded using 50- and 100-ms (note different time scales) test pulses to various potentials (from −80 to +10 mV in 5-mV increments for Kv1.5 and from −100 to +50 mV in 10-mV increments for Kv2.1) followed by a pulse to −40 mV. Further explanations are in the text

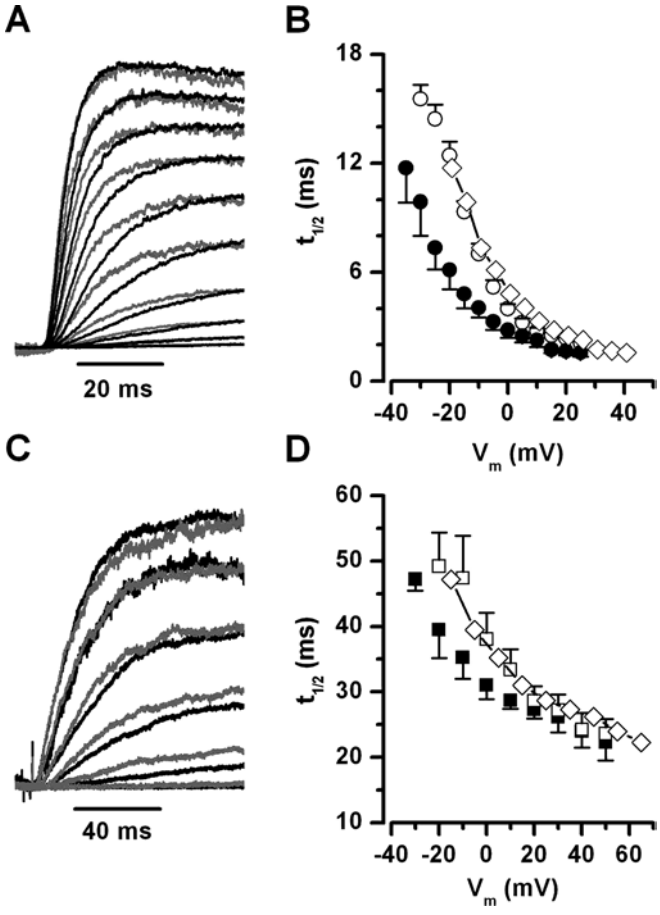

Fig. 2A–D Effect of $Mg^{2+}{}_i$ on the current-activation kinetics. Kv1.5 (**A**) and Kv2.1 (**C**) currents are compared at test potentials between −35 and +10 mV every 5 mV (Kv1.5) and between –50 and + 50 mV in 20-mV steps (Kv2.1) recorded from the same patches in the absence (*black lines*) and in the presence of 10 mM $Mg^{2+}{}_i$ (*grey lines*). To facilitate the comparison, the currents were normalized to the maximum current measured at +10 (Kv1.5) and +50 mV (Kv2.1) and superimposed. Note the difference in the time scales. For Kv1.5 (**B**) and Kv2.1 (**D**), the potential-dependence of the mean $t_{1/2}$ (recorded from 5–23 different patches) in the absence (*open circles* and *squares*) and in the presence of 10 mM $Mg^{2+}{}_i$ (*filled symbols*) is compared. *Diamonds* show $t_{1/2}$ values measured in the presence of 10 mM $Mg^{2+}{}_i$ but corrected for the mean-shift in the steady-state activation dependencies as described in the text

comparison shows a leftward shift in the potential-dependence of $t_{1/2}$ for both channel types, although the effect on $t_{1/2}$ of Kv1.5 current was more prominent. Also, differences in the activation kinetics become less apparent at positive membrane voltages (Fig. 2).

$Mg^{2+}{}_i$-dependent changes in the steady-state activation of Kv1.5 and Kv2.1 channels

One possible explanation for such differences in the activation kinetics could be a negative shift in the steady-state activation dependence produced by an increased concentration of divalent cations including $Mg^{2+}{}_i$ (Perozo and Bezanilla 1991). Therefore, steady-state activation dependencies for the Kv1.5 and Kv2.1 currents were constructed from the instantaneous current–voltage [$I(V)$] relationships. $I(V)$s were measured using a two-step voltage protocol: a pre-pulse applied to different membrane voltages followed by a 20-ms test pulse to −40 mV (Fig. 1). The Kv1.5 current was measured by 50-ms depolarizing pre-pulses applied between −80 and +10 mV in 5-mV increments every 2 s. Kv2.1 currents were elicited by 100-ms pre-pulses between −100 and +50 mV in 10-mV increments every 5 s. Under these conditions, the instantaneous current at the beginning of the test pulse was directly proportional to the number of Kv channels opened during the pre-pulse (Moran and Conti 1995). We assumed that due to the short length of the pre-pulses, C-type inactivation, which has a time constant on the order of a few seconds (data not shown), was not substantially developed. $I(V)$s measured in the absence and presence of different concentrations of $Mg^{2+}{}_i$ were normalized, plotted against the test-pulse potential and fitted with the Boltzmann equation:

$$\frac{I}{I_{\max}} = \frac{1}{1 + \exp\left[-(V - V_a)/k_a\right]} \quad (1)$$

where I/I_{max} is the normalized instantaneous current measured at the beginning of the test pulse, V_a is the half-activation potential, and k_a is the maximum e-fold slope of the activation curve. $I(V)$ dependencies for the Kv1.5 and Kv2.1 currents recorded from the same representative membrane patches in the absence and presence of 5 and 10 mM $Mg^{2+}{}_i$ are compared in Fig. 3. The analysis of Mg^{2+} dependency of the mean values of V_a (Table 1) shows a significant shift by 15 and 16.1 mV to more negative membrane voltages for the Kv1.5 and Kv2.1 channels respectively within the range of concentrations of the cation used in this study (0–10 mM). No significant effect on the slope of activation was observed for different concentrations of $Mg^{2+}{}_i$ (Table 1).

A 15- to 16-mV leftward shift in the activation dependencies of both Kv channels could be potentially responsible for the observed acceleration of current kinetics. To test this possibility, the average $t_{1/2}$ values of Kv1.5 and Kv2.1 currents measured at each membrane potential in 10 mM $Mg^{2+}{}_i$ were corrected for the mean shifts in the activation dependencies ($\Delta V_a = 15$ and 16.1 mV, respectively) and plotted as diamonds in Fig. 2B, D. The comparison showed virtually complete overlap between the corrected $t_{1/2}$ values obtained in 10 mM $Mg^{2+}{}_i$ and those obtained in the absence of Mg^{2+}, strongly suggesting that the change in the rate of the Kv1.5 and Kv2.1 current kinetics was entirely due to Mg^{2+}-induced shifts in the steady-state activation dependencies.

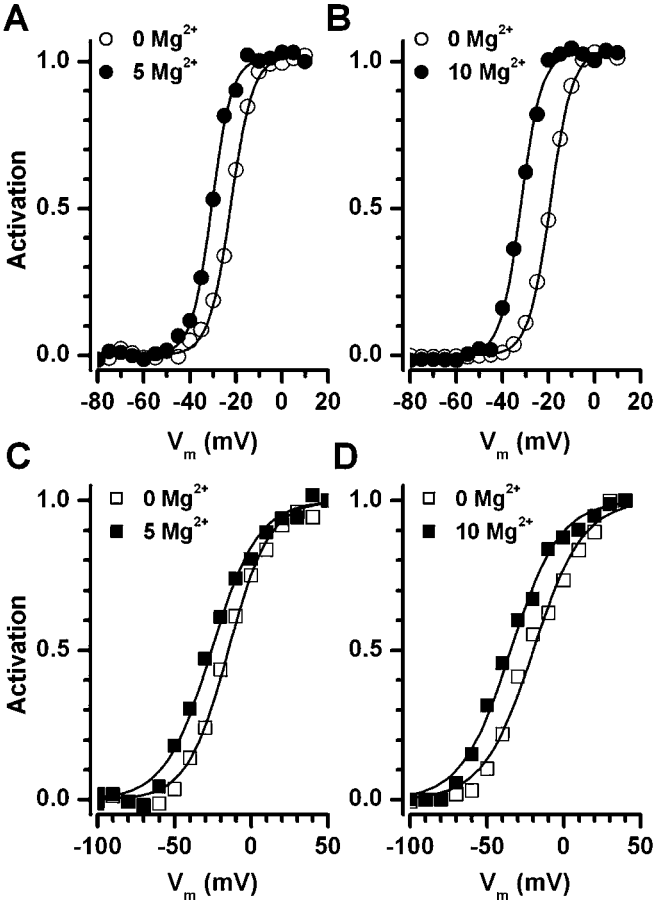

Fig. 3 Effect of $Mg^{2+}{}_i$ on the steady-state activation dependency of the Kv1.5 (**A** and **B**) and Kv2.1 (**C** and **D**) channels recorded in paired inside-out membrane patches. *Continuous lines* are the fit to the Boltzmann equation [Eq. (1)] with V_a equal to −22.3 and −30.6 mV (**A**), −19.2 and −32 mV (**B**), −15 and −25.9 mV (**C**), and −20 and −34.7 mV (**D**) in the absence and the presence of 5 (**A** and **C**) and 10 (**B** and **D**) $Mg^{2+}{}_i$ respectively. Corresponding values of k_a were 4.8 and 4.4 mV (**A**), 4.8 and 4.4 mV (**B**), 13.4 and 15.2 mV (**C**), and 16.3 and 16 mV (**D**)

Effect of $Mg^{2+}{}_i$ on Kv1.5 and Kv2.1 inactivation

The inactivation of the Kv1.5 and Kv2.1 channels was evaluated as the channel availability after a 10-s conditioning depolarization (V_c) applied between −80 and 0 mV (Kv1.5) and between −120 and −40 mV (Kv2.1). The peak current amplitude (I_p), measured at the subsequent test pulse to +60 mV, was normalized to that recorded after most negative V_c (I_{max}), and fitted with the following function:

$$\frac{(I_p - I_{ss})}{(I_{max} - I_{ss})} = \frac{1}{(1 + \exp(V_c - V_h)/k_h)} \quad (2)$$

where I_{ss} is the asymptotic non-inactivating current at the most depolarized V_c, V_h is the half-inactivation potential, and k_h is the maximum e-fold slope of inactivation. Figure 4 compares the representative inactivation dependencies for Kv1.5 (A and B) and Kv2.1 (C and D) recorded from the same patches in the absence and after addition of 5 or 10 mM $Mg^{2+}{}_i$, respectively. Similarly to the steady-state activation, an increase in $Mg^{2+}{}_i$ caused progressive leftward shift in availabilities of both Kv currents reaching ~13 mV in 10 mM $Mg^{2+}{}_i$, without significant effect on k_h (Table 1).

Interestingly, in the presence of 10 mM $Mg^{2+}{}_i$ the non-inactivating I_{ss} fraction was significantly reduced by ~50% ($P < 0.001$) for the Kv1.5, but not for the Kv2.1 current (Fig. 4 and Table 1). The incomplete inactivation observed for the Kv1.5 current may reflect a kinetic equilibrium between the inactivated and the open states of the channel (Marom et al. 1993; Bertoli et al. 1996; Marom 1998), which could be modified by $Mg^{2+}{}_i$, favouring the inactivated state. In this case, one would expect a greater use-dependency of the Kv1.5, but not the Kv2.1 current, in the presence of high $Mg^{2+}{}_i$ due to a faster accumulation of inactivation. To analyze this effect, membrane patches containing Kv channels were stimulated by depolarizing pulses to +20 mV in different concentrations of $Mg^{2+}{}_i$ with frequency of 0.5 (Kv1.5) or 0.3 Hz (Kv2.1). Figure 5 shows the time and $Mg^{2+}{}_i$ dependence of the mean Kv1.5 peak current recorded with this protocol. As can be seen, an increase in $Mg^{2+}{}_i$ progressively accelerated a monoexponential decrease in the current amplitude with time constants equal to 66, 46 and 23 s in the absence and in the presence of 5 and 10 mM $Mg^{2+}{}_i$ respectively. The steady-state level of Kv1.5 current amplitude was sig-

Table 1 Comparison of steady-state activation and inactivation parameters for the Kv1.5 and Kv2.1 channels in different concentrations of $Mg^{2+}{}_i$. Data represent mean ± SEM (number of experiments is given in parentheses). V_a, k_a, V_h, k_h and I_{ss} are defined in the text. *Asterisks* indicate significant differences between given values and those measured in the absence of Mg^{2+}

$[Mg^{2+}]_i$ (mM)	V_a (mV)	k_a (mV)	V_h (mV)	k_h (mV)	I_{ss}
Kv1.5 channel					
0	−22.9 ± 1.3 (7)	−4.5 ± 0.8 (7)	−37.3 ± 1.5 (12)	3.6 ± 0.2 (12)	0.22 ± 0.02 (12)
5	−31.4 ± 2.2 (3)*	−4.4 ± 0.5 (3)	−45.2 ± 2.5 (8)*	4.2 ± 0.6 (8)	0.12 ± 0.01 (8)*
10	−37.9 ± 1.2 (4)*	−3.9 ± 0.7 (4)	−50.9 ± 1.8 (4)*	3.4 ± 0.1 (4)	0.10 ± 0.02 (4)*
Kv2.1 channel					
0	−11.8 ± 2.7 (9)	−16.0 ± 1.2 (9)	−80.1 ± 4.6 (6)	8.3 ± 0.3 (6)	0.02 ± 0.02 (6)
5	−18.0 ± 1.7 (4)*	−16.7 ± 2.0 (4)	−84.2 (1)	8.9 (1)	0.0 (1)
10	−27.9 ± 1.2 (5)*	−16.7 ± 1.1(5)	−93.1 ± 5.8 (5)*	8.1 ± 1.7 (5)	0.02 ± 0.01 (5)

nificantly reduced by 13 ± 1% ($n = 5$) and 24 ± 1% ($n = 7$) in 5 and 10 mM $Mg^{2+}{}_i$ respectively ($P < 0.0001$), compared to 6 ± 3% reduction in 21 patches seen in $Mg^{2+}{}_i$-free solution. For the Kv2.1 channels, on the other hand, no $Mg^{2+}{}_i$-dependent potentiation of the current reduction was observed. The peak current was equally suppressed by 28.7 ± 4.6% ($n = 3$) and by 27.9 ± 6.2% ($n = 3$) after 60 s of stimulation in 0 and 10 mM $Mg^{2+}{}_i$ respectively (data not shown).

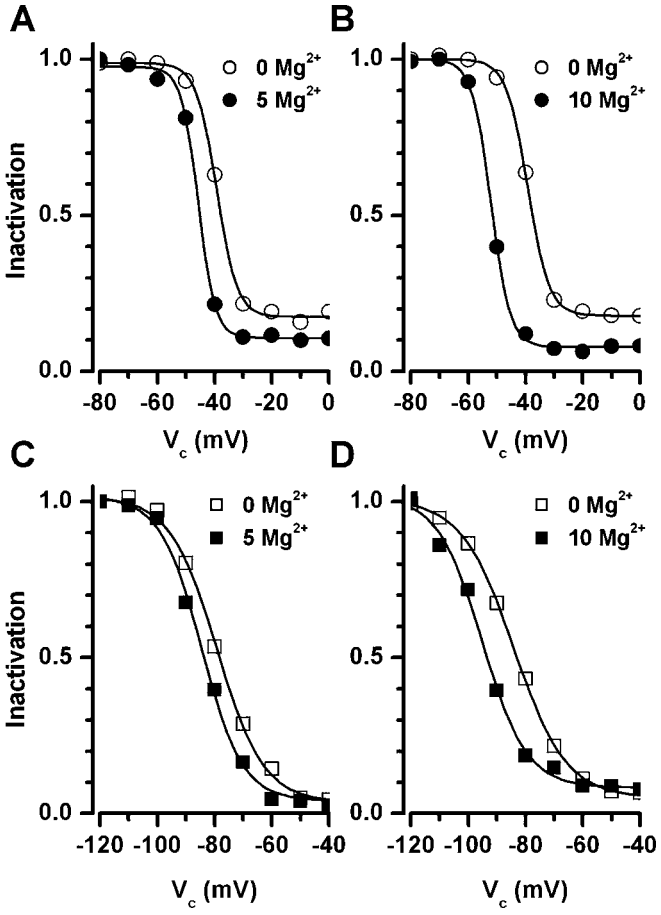

Fig. 4 Effect of $Mg^{2+}{}_i$ on inactivation of Kv1.5 (**A** and **B**) and Kv2.1 (**C** and **D**). *Continuous lines* are the fit to the Boltzmann equation [Eq. (2)] with V_h equal to −39.3 and −45.7 mV (**A**), −39.3 and −52 mV (**B**), −79.1 and −84.5 mV (**C**), and −84.1 and −95.1 mV (**D**) in the absence and the presence of 5 (**A** and **C**) and 10 (**B** and **D**) $Mg^{2+}{}_i$, respectively. Corresponding values of k_h were 3.6 and 3 mV (**A**), 3.7 and 3.3 mV (**B**), 8.2 and 7.2 mV (**C**), and 9.2 and 7.8 mV (**D**). The non-inactivating component I_{ss} was changed from 0.17 to 0.11 (**A**) and from 0.18 to 0.08 (**B**) for the Kv1.5 current, while remaining unaltered for the Kv2.1 at 0.04 (**C**) for both dependencies, and 0.05 and 0.08 in the absence and presence of 10 mM $Mg^{2+}{}_i$ (**D**)

Role of fixed negative charges

Similar shifts in the activation and inactivation dependencies of Kv1.5 and Kv2.1 channels suggest that voltage gating of both channels is similarly affected by $Mg^{2+}{}_i$ possibly via interaction with negative charges in the vicinity of the voltage sensor of the channel. It is well known that divalent cations can "screen" the surface charges by forming an ionic diffuse double layer at the surface or by binding to them forming complexes. Both effects will reduce the negative surface potential. Hence, divalent cations added intracellularly will decrease membrane depolarization required to bring the voltage field within the membrane to a given value. Changes in surface potential in different concentrations of divalent cations can be described using the Gouy-Chapman model (see Hille 2001 for comprehensive review and references therein). According to the model, the measured membrane potential (V_m) between the intra- and extracellular compartments is composed of the outer surface potential (ψ_o), the actual transmembrane potential (V^*) and the inner surface potential (ψ_i):

$$V_m = V^* + \psi_o - \psi_i \tag{3}$$

Since ψ_o is constant under our experimental conditions, then $\psi_o + V^* = E$ can also be considered as a constant. Setting $V_m = V_a$, the $Mg^{2+}{}_i$-dependent changes in V_a will therefore represent corresponding changes in ψ_i according to:

$$V_a = E - \psi_i \tag{4}$$

The dependence of ψ_i on the concentration of $Mg^{2+}{}_i$ can then be described with the Grahame equation:

$$\sigma^2 = 2\varepsilon\varepsilon_0 RT\left[\sum_j C_j\left(\exp\frac{-z_j F\psi_i}{RT} - 1\right)\right] \tag{5}$$

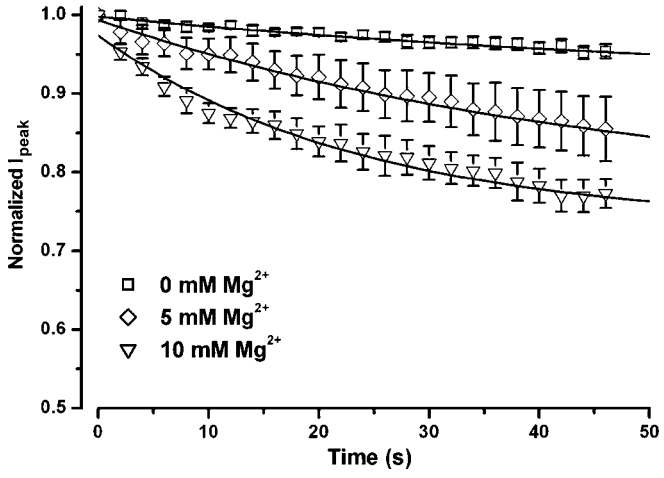

Fig. 5 Time- and Mg^{2+}-dependent inhibition of the Kv1.5 current. Membrane patches were stimulated every 2 s in different concentrations of $Mg^{2+}{}_i$ as indicated. The Kv1.5 peak amplitude was normalized to that recorded during the first pulse. *Continuous lines* represent single exponential fits with time constants of 63, 46 and 23 s for 0 ($n=21$), 5 ($n=5$) and 10 ($n=5$) mM $Mg^{2+}{}_i$ respectively

where ε_0 is the polarizability of free space, ε is the dielectric constant of the aqueous intracellular solution, σ is the surface-charge density, and C_j is the concentration of the jth internal ionic species of valence z_j. R, T and F have their usual meanings. Figure 6 shows the values of ΔV_a (circles) and ΔV_h (diamonds) for the Kv1.5 (open symbols) and the Kv2.1 (filled symbols) currents plotted against free $Mg^{2+}{}_i$ (note a reduced amount of free $Mg^{2+}{}_i$ compared to the total added Mg^{2+} due to the presence of 2 mM EGTA). The continuous line represents an evaluation of Eq. (5), with $\sigma = 1$ e$^-$/100 Å^2, a value determined by a minimum least-square approach, that better describes our experimental data.

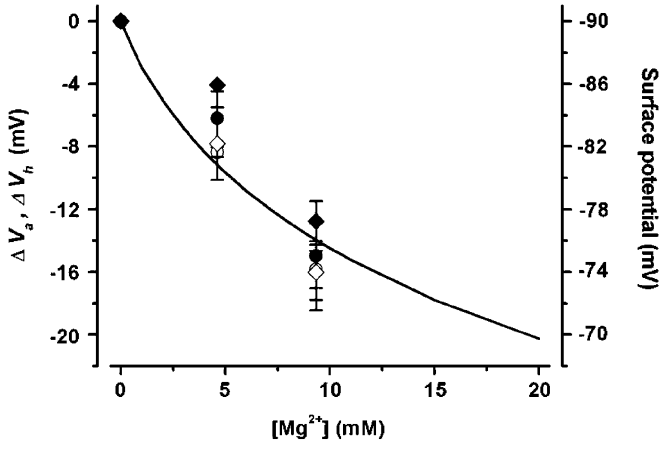

Fig. 6 Interpretation of $Mg^{2+}{}_i$-induced changes in activation and inactivation dependencies with the Gouy-Chapman formalism. The mean relative shifts in the half-activation (ΔV_a, *circles*) and half-inactivation (ΔV_h, *diamonds*) potentials for the Kv1.5 (*open symbols*) and Kv2.1 (*filled symbols*) channels were plotted against the calculated free $Mg^{2+}{}_i$. The *continuous line* represents numerical solution of the Grahame equation [Eq. (5)] with $\delta = 1$ e$^-$/100 Å^2. The *right axis* shows the values of the estimated surface potentials. Further explanations are in the text

Comparison of the voltage-dependent block of Kv1.5 and Kv2.1 channels by $Mg^{2+}{}_i$

Reduction in the Kv current amplitude observed with increased $Mg^{2+}{}_i$ is likely to be due to a voltage-dependent block described previously for a variety of cloned mammalian Kv channels (Ludewig et al. 1993; Slesinger et al. 1993; Lopatin and Nichols 1994; Harris and Isacoff 1996; Gomez-Hernandez et al. 1997), including the Kv2.1 (Lopatin and Nichols 1994). Interestingly, the effect of $Mg^{2+}{}_i$ on the Kv1.5 channel current has not been studied yet. We therefore compared the voltage-dependent block of the Kv1.5 and Kv2.1 instantaneous currents by $Mg^{2+}{}_i$ using the following voltage protocol. Near-maximum activation of the Kv1.5 and Kv2.1 channels was achieved by a 20- or 100-ms step respectively, membrane depolarization to +20 mV followed by repolarization to various test potentials between −100 and +70 mV and between −90 and +100 mV in 10-mV increments for the Kv1.5 (0.5 Hz) and Kv2.1 (0.2 Hz) currents respectively. The instantaneous tail current at each test pulse was fitted to a single exponential, and its amplitude was obtained from extrapolation of the fit to the beginning of the test pulse. The tail current measured in the presence of $Mg^{2+}{}_i$ was then normalized to the current measured at the end of the pre-pulse in the absence of Mg^{2+}. Figure 7A, C shows families of representative tail currents recorded from representative membrane patches expressing Kv1.5 (A) and Kv2.1 (C) in the absence and presence of 10 mM $Mg^{2+}{}_i$. Figure 7B, D compares the averaged normalized instantaneous tail-current voltage relationships, $I_t(V)$, recorded in 0 and 10 mM $Mg^{2+}{}_i$ for Kv1.5 and in 0, 5, and 10 mM $Mg^{2+}{}_i$ for Kv2.1. This comparison shows that an increase in $Mg^{2+}{}_i$ produces a greater rectification of the Kv2.1 current than the Kv1.5 current.

Since the Goldman-Hodgkin-Katz formalism was not applicable in this case due to current rectification occurring at positive potentials (>50 mV) even in the absence of $Mg^{2+}{}_i$, the $I_t(V)$ in the absence of $Mg^{2+}{}_i$, $I_t(0,V)$, was interpolated with a third-order polynomial function, which is independent of any model assumption. $I_t(V)$ in the presence of different concentrations of $Mg^{2+}{}_i$, $I_t([Mg^{2+}],V)$, was described by combining a third-order polynomial function describing the voltage dependence of the tail current in the absence of $Mg^{2+}{}_i$, $I_t(0,V)$, and a factor, $B([Mg^{2+}],V)$, characterizing the probability of the channel block as a function of the Mg^{2+} concentration and membrane potential:

$$I_t\left(\left[Mg^{2+}\right],V\right) = I_t(0,V) \times B\left(\left[Mg^{2+}\right],V\right) \quad (6)$$

where $B([Mg^{2+}],V)$ can be expressed in a way similar to that described previously in Woodhull (1973):

$$B_{Mg}\left(\left[Mg^{2+}\right],V\right) = \frac{1}{1+\frac{\left[Mg^{2+}\right]}{K_d(0)\exp\left(z\delta FV/RT\right)}} \quad (7)$$

where $K_d(0)$ is the apparent dissociation constant for Mg^{2+} defined at $V=0$, $z=2$ is the valence of Mg^{2+}, δ is

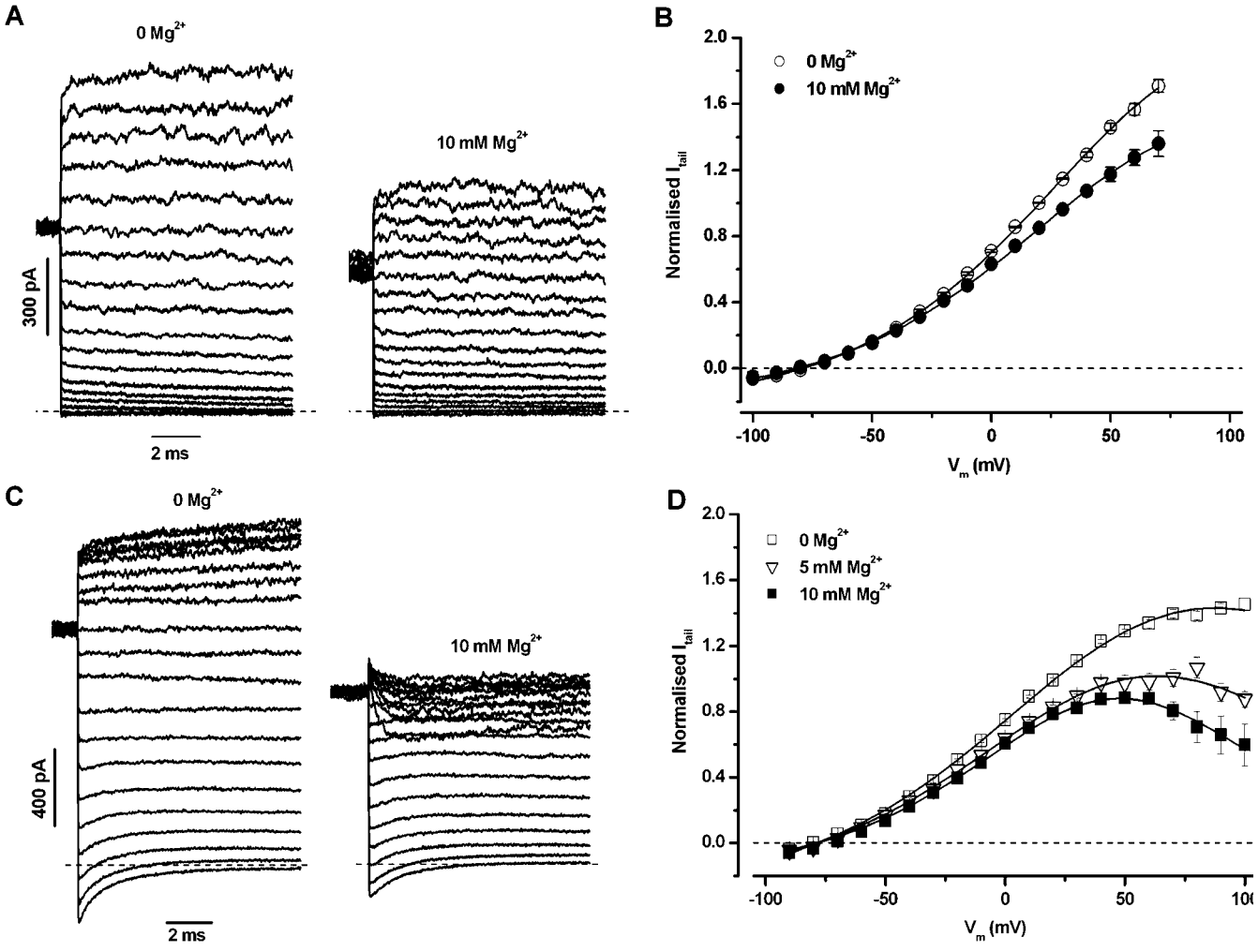

Fig. 7 Voltage dependency of the $Mg^{2+}{}_i$ block of Kv1.5 (**A** and **B**) and Kv2.1 (**C** and **D**) channels. Families of tail currents were recorded during test potentials applied in 10-mV increments from −100 to +70 mV (Kv1.5, **A**) and from −90 to +100 mV (Kv2.1, **C**) after a pre-pulse to +20 mV in the absence and presence of 10 mM $Mg^{2+}{}_i$, as indicated. *Dashed lines* represent zero current. **B** and **D** compare the mean tail current at each test potential normalized to the current at the end of pre-pulse for Kv1.5 (**B**) and Kv2.1 (**D**) channels in the presence of different $Mg^{2+}{}_i$ as indicated. Data represent the mean of 5–11 recordings obtained from different patches. *Continuous lines* represent the fit with Eq. (7). See text for further explanations

the relative electric distance of Mg^{2+}-binding site from the internal surface of the cell membrane, and R, T and F have their usual meanings. The fit of the averaged tail current obtained at different concentrations of $Mg^{2+}{}_i$ (shown in Fig. 7B, D) using Eq. (7) gave a value of $K_d(0) = 68.1 \pm 2.5$ mM and $\delta = 0.11 \pm 0.02$ for the Kv1.5 channels, and $K_d(0) = 43.4 \pm 2.8$ mM and $\delta = 0.21 \pm 0.04$ for the Kv2.1 ($P < 0.01$).

Alternatively, $K_d(0)$ and δ can also be calculated from the estimation of K_d at each membrane potential, $K_d(V)$, according to the Michaelis-Menten equation. Resulting values of $K_d(V)$ estimated for Kv1.5 and Kv2.1 at $Mg^{2+}{}_i = 10$ mM were plotted against the membrane potential in Fig. 8 and approximated with the following equation (Woodhull 1973):

$$K_d(V) = K_d(0) \exp\left(\frac{-\delta z V F}{RT}\right) \quad (8)$$

The satisfactory fit of individual $K_d(V)$ at each membrane voltage (solid lines in Fig. 8) was achieved at $K_d(0) = 70.0 \pm 2.5$ mM and $\delta = 0.11 \pm 0.05$ for the Kv1.5, and $K_d(0) = 40.5 \pm 1.7$ mM and $\delta = 0.19 \pm 0.08$ for the Kv2.1, which are close to the values estimated with Eq. (7). These results suggest that a putative Mg^{2+}-binding site in the Kv2.1 has a higher affinity than that in the Kv1.5 channels and is situated twice as deep in the membrane electric field, explaining a greater voltage dependence of the Mg^{2+} block of the Kv2.1 current.

Discussion

An increase in $Mg^{2+}{}_i$ concentration had several distinct effects on the Kv1.5 and Kv2.1 channels heterologously expressed in *Xenopus* oocytes, including the inhibition of the current amplitude due to a potential-dependent block of the currents by intracellular magnesium, the apparent

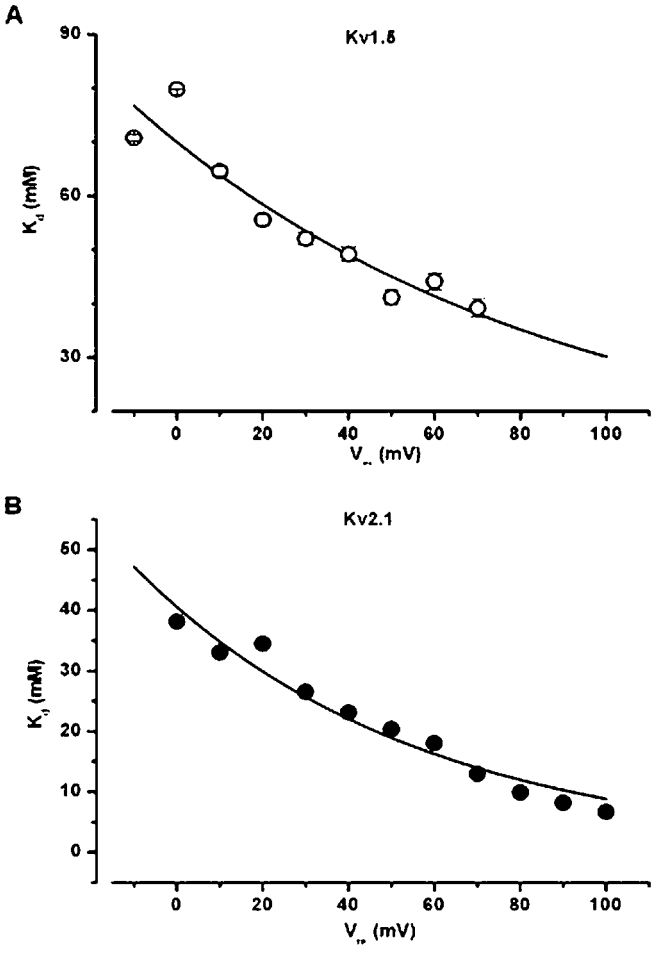

Fig. 8 Potential-dependence of K_d of the block of *Kv1.5* (**A**) and *Kv2.1* (**B**) channel currents by $Mg^{2+}{}_i$. K_d was calculated at each membrane potential as described in the text. *Continuous lines* represent the fit with Eq. (8)

acceleration of the current kinetics of activation associated with the leftward shift of the steady-state activation dependencies, and the significant shift of inactivation dependencies to more negative membrane voltages.

The block of Kv channels by intracellular Na^+, tetraethylammonium (TEA), Ba^{2+} and Mg^{2+} has been used extensively as a tool to investigate pore–ion interactions (Ludewig et al. 1993; Slesinger et al. 1993; Lopatin and Nichols 1994; Harris and Isacoff 1996; Gomez-Hernandez et al. 1997). The results of these studies demonstrated a strong voltage dependence of the block of various Kv channel isoforms by intracellular Na^+, Ba^{2+} and Mg^{2+}, while TEA-dependent block was only weakly dependent on membrane voltage (Ludewig et al. 1993; Slesinger et al. 1993; Lopatin and Nichols 1994; Harris and Isacoff 1996; Gomez-Hernandez et al. 1997), thus indicating that cations, but not TEA, bind relatively deep within the permeation pathway of the channel. Our results also confirmed that Mg^{2+} blocks the Kv1.5 and Kv2.1 channels in a voltage-dependent manner with $K_d(0)$ equal to ~70 and 40 mM and the calculated electrical distance of the Mg^{2+}-binding site equal to 0.11 and 0.21, respectively. The latter values are close to values of δ (0.28–0.38) reported for several members of the Kv1 subfamily (Ludewig et al. 1993) and the Kv2.1 (Lopatin and Nichols 1994) and Kv3.1 (Harris and Isacoff 1996) channels. However, the value of K_d for the Kv2.1 calculated at +50 mV (20.4 mM) was approximately four times higher than $K_d(50)$ of 4.8 mV reported in Lopatin and Nichols (1994). Similar discrepancies in K_d values have been described for Kv1.1 and Kv1.4 channel currents (Ludewig et al. 1993; Gomez-Hernandez et al. 1997) and explained by the differences in the experimental conditions, particularly in the external K^+ concentration which is known to affect the Mg^{2+}-binding affinity (Ludewig et al. 1993; Lopatin and Nichols 1994; Gomez-Hernandez et al. 1997). In addition, the value of $K_d(0)$ for Kv1.5 and Kv2.1 channels in our experiments may also be underestimated due to the presence of Tris in the bath solution, which has been shown to block K^+ channels in a voltage-dependent manner (Coronado and Miller 1982) and therefore might be responsible for some rectification observed in the absence of Mg^{2+}. Nevertheless, a direct comparison of the voltage dependence of the block of the Kv1.5 and Kv2.1 channels (which possess distinct electrophysiological and pharmacological properties) recorded under the same experimental conditions demonstrated that the potency and the voltage-sensitivity of the block were significantly greater for the Kv2.1 than for the Kv1.5 channel. Further experimentation will be required to identify the exact location of binding sites responsible for these differences.

An increase in $Mg^{2+}{}_i$ also caused a marked effect on the current activation kinetics, which accelerated for both types of Kv currents, shifting the dependence of the half-time of activation to the left. The removal of these apparent differences in the current kinetics by a simple correction of the voltage dependency of $t_{1/2}$ for the mean-shifts in the Kv1.5 and Kv2.1 steady-state activation dependencies indicates that changes in $Mg^{2+}{}_i$ also modulate the Kv channel gating. Although the effect of extracellular Mg^{2+} (as well as other divalent cations) on the voltage-dependent characteristics of various heterologously expressed Kv channels has been previously investigated (Elinder et al. 1996, 1998; Elinder and Arhem 1999), the effect of intracellular Mg^{2+} on the gating mechanisms of the expressed Kv channel had not been characterized previously. Our comparison of Mg^{2+}-dependent changes in the steady-state mid-activation and mid-inactivation parameters suggests that both gating mechanisms in the two distinctive Kv channel subtypes "see" Mg^{2+} similarly. Traditionally, such behavior for various channel types has been interpreted as an interaction of divalent cations with fixed negative charges situated in close vicinity to the ion-channel voltage sensor (Hille 2001). Application of the Gouy-Chapman formalism (assuming that $Mg^{2+}{}_i$ can only screen the fixed charges) yielded an estimated density of 1 negative charge per 100 $Å^2$ or 1 e^-/nm^2. This value is close to values re-

ported for the intracellular charge density in the squid axon Kv channels (0.29–0.63 e^-/nm^2) (Perozo and Bezanilla 1991), but was approximately six times smaller than that of the extracellular charge density of the expressed Kv1.4 and Kv2.1 channels (0.17 e^-/nm^2) (Elinder and Arhem 1999). The exact nature of fixed charges which sense the presence of $Mg^{2+}{}_i$ is not known; however, by analogy with the extracellular charges (Elinder and Arhem 1999; Elinder et al. 2001), fixed charges are likely to form part of the Kv channel molecule. It should be noted that the density of the surface charges (which "sense" $Mg^{2+}{}_i$) on the Kv channel in the squid axon was altered differentially by conditions favoring phosphorylation, increasing to a greater extent for the inactivation than for the activation dependencies (Perozo and Bezanilla 1991). Such a differential effect can have important physiological consequences by altering the number of Kv channels available at each membrane potential. Indeed, voltage-dependent activation and inactivation are modulated differently by an increase in $Mg^{2+}{}_i$ arterial myocytes isolated from the rat main pulmonary artery and from the rat aorta, which express different types of Kv currents (Tammaro and Smirnov 2003).

Interestingly, despite a similar leftward shift in the activation and inactivation dependencies for both Kv channel subtypes, a significant inhibition of more than 50% of the non-inactivating fraction of the Kv1.5 current, but not the Kv2.1, by increased $Mg^{2+}{}_i$ was demonstrated, suggesting the Kv1.5 channel favours the inactivated state in high concentrations of $Mg^{2+}{}_i$. The Mg^{2+}-dependent increase in accumulation of inactivation of the Kv1.5, and not the Kv2.1 channel, is in agreement with this observation (Fig. 5). Notably, a similar effect of $Mg^{2+}{}_i$ on the non-inactivating component of the native Kv current, which is thought to be mediated at least in part by the Kv1.5 channel subunit (Smirnov et al. 2002), was also observed in one subpopulation of myocytes isolated from the rat main pulmonary artery. Although the understanding of the mechanism of this effect requires further experimental support, a possible interaction cannot be excluded between the effect of $Mg^{2+}{}_i$ on the permeation mechanism of the open Kv1.5 channel and the C-type inactivation, whose apparent voltage dependence is given by the voltage-dependent process of activation and is thought to occur as a result of the constriction of the outer mouth of the permeation pore (Pardo et al. 1992; Lopez-Barneo et al. 1993; Yellen 1998). Interestingly, a number of mutations in the S4-S5 intracellular loop of the *Shaker* channel significantly altered the sensitivity of the channel to intracellular TEA, Ba^{2+} and Mg^{2+} (Slesinger et al. 1993), supporting a possible involvement of distal parts of the channel in the Mg^{2+}-dependent modulation of the Kv currents.

In conclusion, we have demonstrated that an increase in $Mg^{2+}{}_i$ caused significant changes in both the channel gating and permeation mechanisms of two distinct types of Kv channels, Kv1.5 and Kv2.1. The $Mg^{2+}{}_i$-induced changes in the channel steady-state activation and inactivation dependencies and the selective inhibition of the non-inactivating component of the Kv1.5, but not the Kv2.1, may play an important physiological role in the regulation of the function of cells expressing these channel subtypes.

Acknowledgements The cDNA for the Kv2.1 channel was kindly provided by Dr. R. Joho. This work was supported by the British Heart Foundation (grant FS/20000013) and FISR-MIUR, Italy.

References

Bertoli A, Moran O, Conti F (1996) Accumulation of long-lasting inactivation in rat brain K^+ channels. Exp Brain Res 110:401–412

Coronado R, Miller C (1982) Conduction and block by organic cations in a K^+-selective channel from sarcoplasmic reticulum incorporated into planar phospholipid bilayers. J Gen Physiol 79:529–547

Elinder F, Arhem P (1999) Role of individual surface charges of voltage-gated K channels. Biophys J 77:1358–1362

Elinder F, Arhem P, Larsson HP (2001) Localization of the extracellular end of the voltage sensor S4 in a potassium channel. Biophys J 80:1802–1809

Elinder F, Liu Y, Arhem P (1998) Divalent cation effects on the *Shaker* K channel suggest a pentapeptide sequence as determinant of functional surface charge density. J Membr Biol 165:183–189

Elinder F, Madeja M, Arhem P (1996) Surface charges of K channels. Effects of strontium on five cloned channels expressed in *Xenopus* oocytes. J Gen Physiol 108:325–332

Frech GC, VanDongen AM, Schuster G, Brown AM, Joho RH (1989) A novel potassium channel with delayed rectifier properties isolated from rat brain by expression cloning. Nature 340:642–645

Friel DD, Tsien RW (1989) Voltage-gated calcium channels: direct observation of the anomalous mole fraction effect at the single-channel level. Proc Natl Acad Sci USA 86:5207–5211

Gomez-Hernandez JM, Lorra C, Pardo LA, Stuhmer W, Pongs O, Heinemann SH, Elliott AA (1997) Molecular basis for different pore properties of potassium channels from the rat brain Kv1 gene family. Pflügers Arch 434:661–668

Hamill O, Marty A, Neher E, Sakmann B, Sigworth F (1981) Improved patch-clamp techniques for high resolution current recording from cells and cell-free membrane patches. Pflügers Arch 391:85–100

Harris RE, Isacoff EY (1996) Hydrophobic mutations alter the movement of Mg^{2+} in the pore of voltage-gated potassium channels. Biophys J 71:209–19

Hille B (2001) Ionic channels of excitable membranes. Sinauer, Sunderland, MA

Hoshi T, Zagotta WN, Aldrich RW (1991) Two types of inactivation in *Shaker* K^+ channels: effects of alterations in the carboxy-terminal region. Neuron 7:547–556

Kerschensteiner D, Monje F, Stocker M (2003) Structural determinants of the regulation of the voltage-gated potassium channel Kv2.1 by the modulatory alpha-subunit Kv9.3. J Biol Chem 278:18154–161

Klemic KG, Shieh CC, Kirsch GE, Jones SW (1998) Inactivation of Kv2.1 potassium channels. Biophys J 74:1779–1789

Lin F, Conti F, Moran O (1991) Competitive blockage of the sodium channel by intracellular magnesium ions in central mammalian neurones. Eur Biophys J 19:109–118

Lopatin AN, Nichols CG (1994) Internal Na^+ and Mg^{2+} blockade of DRK1 (Kv2.1) potassium channels expressed in *Xenopus* oocytes. Inward rectification of a delayed rectifier. J Gen Physiol 103:203–216

Lopez-Barneo J, Hoshi T, Heinemann SH, Aldrich RW (1993) Effects of external cations and mutations in the pore region on C-type inactivation of *Shaker* potassium channels. Receptors Channels 1:61–71

Ludewig U, Lorra C, Pongs O, Heinemann SH (1993) A site accessible to extracellular TEA and K^+ influences intracellular Mg^{2+} block of cloned potassium channels. Eur Biophys J 22:237–47

Marom S (1998) Slow changes in the availability of voltage-gated ion channels: effects on the dynamics of excitable membranes. J Membr Biol 161:105–113

Maron S, Goldstein SAN, Kupper J, Levitan IB (1993) Mechanism and modulation of inactivation of the Kv3 potassium channel. Receptors Channels 1:81–88

Matsuda H (1991) Magnesium gating of inwardly rectifying K^+ channel. Annu Rev Physiol 53:289–98

Moran O, Conti F (1995) Properties of the Kv1.1 rat brain potassium channels expressed in mammalian cells: temperature effects. Biochem Biophys Res Commun 215:915–920

Pardo LA, Heinemann SH, Terlau H, Ludewig U, Lorra C, Pongs O, Stühmer W (1992) Extracellular K^+ specifically modulates a rat brain K^+ channel. Proc Natl Acad Sci USA 89:2466–2470

Perozo E, Bezanilla F (1991) Phosphorylation of K^+ channels in the squid giant axon. A mechanistic analysis. J Bioenerg Biomembr 23:599–613

Pusch M (1990) Open-channel block of Na^+ channels by intracellular Mg^{2+}. Eur Biophys J 18:317–326

Pusch M, Conti F, Stühmer W (1989) Intracellular magnesium blocks sodium inward currents in a voltage- and dose-dependent manner. Biophys J 55:1267–1271

Slesinger PA, Jan YN, Jan LY (1993) The S4-S5 loop contributes to the ion-selective pore of potassium channels. Neuron 11:739–49

Smirnov SV, Beck R, Tammaro P, Ishii T, Aaronson PI (2002) Electrophysiologically distinct smooth muscle cell subtypes in rat conduit and resistance pulmonary arteries. J Physiol 538:867–878

Snyders DJ, Tamkun MM, Bennett PB (1993) A rapidly activating and slowly inactivating potassium channel cloned from human heart. Functional analysis after stable mammalian cell culture expression. J Gen Physiol 101:513–543

Tammaro P, Smirnov SV (2003) Modulation of the voltage-gated potassium (Kv) channel currents by intracellular Mg^{2+} in rat aortic smooth muscle cells (RASMCs). J Physiol C47

Tarr M, Trank JW, Goertz KK (1989) Intracellular magnesium affects I(K) in single frog atrial cells. Am J Physiol 257:H1663–1669

Woodhull AM (1973) Ionic blockage of sodium channels in nerve. J Gen Physiol 61:687–708

Yellen G (1998) The moving parts of voltage-gated ion channels. Q Rev Biophys 31:239–295